plant biology

Plant Biology ISSN 1435-8603

RESEARCH PAPER

Pathogen-induced conditioning of the primary xylem vessels – a prerequisite for the formation of bacterial emboli by *Pectobacterium atrosepticum*

V. Y. Gorshkov[1,2], A. G. Daminova[1], P. V. Mikshina[1], O. E. Petrova[1], M. V. Ageeva[1], V. V. Salnikov[1,2], T. A. Gorshkova[1] & Y. V. Gogolev[1,2]

1 Kazan Institute of Biochemistry and Biophysics, Kazan Scientific Center, Russian Academy of Sciences, Kazan, Russia

2 Kazan Federal University, Kazan, Russia

Keywords

Bacterial emboli; biofilm; *Pectobacterium atrosepticum*; plant cell wall; plant–microbe interaction; reactive oxygen species; rhamnogalacturonan I.

Correspondence

V. Y. Gorshkov, Kazan Institute of Biochemistry and Biophysics, Kazan Scientific Center, Russian Academy of Sciences, Lobachevsky Street 2/31, 420111 Kazan, Russia.

E-mail: gvy84@mail.ru

Editor

W. Adams

Received: 9 January 2016; Accepted: 15 March 2016

doi:10.1111/plb.12448

ABSTRACT

Representatives of *Pectobacterium* genus are some of the most harmful phytopathogens in the world. In the present study, we have elucidated novel aspects of plant–*Pectobacterium atrosepticum* interactions. This bacterium was recently demonstrated to form specific 'multicellular' structures – bacterial emboli in the xylem vessels of infected plants. In our work, we showed that the process of formation of these structures includes the pathogen-induced reactions of the plant. The colonisation of the plant by *P. atrosepticum* is coupled with the release of a pectic polysaccharide, rhamnogalacturonan I, into the vessel lumen from the plant cell wall. This polysaccharide gives rise to a gel that serves as a matrix for bacterial emboli. *P. atrosepticum*-caused infection involves an increase of reactive oxygen species (ROS) levels in the vessels, creating the conditions for the scission of polysaccharides and modification of plant cell wall composition. Both the release of rhamnogalacturonan I and the increase in ROS precede colonisation of the vessels by bacteria and occur only in the primary xylem vessels, the same as the subsequent formation of bacterial emboli. Since the appearance of rhamnogalacturonan I and increase in ROS levels do not hamper the bacterial cells and form a basis for the assembly of bacterial emboli, these reactions may be regarded as part of the susceptible response of the plant. Bacterial emboli thus represent the products of host–pathogen integration, since the formation of these structures requires the action of both partners.

INTRODUCTION

Plant–microbe interactions result in dramatic changes in physiology of both the host and the parasite. Plant responses to pathogen invasion are contingently divided into defence and susceptible responses (O'Donnell *et al.* 2003a; Shan & Goodwin 2006; Uehara *et al.* 2010). The former responses suppress pathogen propagation within the host tissues and the latter make the plant environment more convenient for parasite development. In fact, it is hard to draw the precise line between defence and susceptible reactions of a plant: first, both of these responses are likely controlled by the same regulatory systems (Lund *et al.* 1998; O'Donnell *et al.* 2001; O'Donnell *et al.* 2003a,b Able 2003), and second, a specific reaction of the plant may be either a defence or a susceptible response, depending on the host–pathogen pair, and those reactions that generally confer protection appear to result in susceptibility of the macro-organism to certain pathogens (Govrin & Levine 2000; Greenberg *et al.* 2000; Vogel *et al.* 2002; Cui *et al.* 2005; Lorang *et al.* 2007; Thatcher *et al.* 2009).

A defence response is known to be the result of recognition of the pathogen by the plant (Agrios 2005; Dodds & Rathjen 2010; Spoel & Dong 2012). Otherwise, if recognition does not occur or happens too late to activate protective mechanisms, the plant becomes susceptible. However, it becomes evident that susceptibility is not just passivity of the host but may be regarded as a pathogen-induced response of the plant (Hirsch *et al.* 2002; O'Donnell *et al.* 2003a,b; Mauch-Mani & Mauch 2005; Efetova *et al.* 2007; Robert-Seilaniantz *et al.* 2007). This response entails significant physiological changes that occur in accordance with the scenario of interaction with the pathogen. The lack of such reactions may result in modification of the interaction strategy or even in tolerance or resistance of the host (O'Donnell *et al.* 2003a,b; Nickstadt *et al.* 2004; Laurie-Berry *et al.* 2006; Navarro *et al.* 2006; Ding *et al.* 2008; Zheng *et al.* 2012).

Defence and susceptible responses are poorly understood for plant–*Pectobacterium* pathosystems. *Pectobacterium* species are well-known necrotrophic phytopathogens that belong to the soft-rot *Enterobacteriaceae* (SRE) group of microorganisms. These bacteria cause soft-rot and blackleg diseases in plants (Bain *et al.* 1990; Perombelon 2002; Toth *et al.* 2003; Czajkowski *et al.* 2011; Charkowski *et al.* 2012). Up to now, no plant genes that determine the resistance to SRE have been

identified. The questions about the susceptible response of plants to *Pectobacterium* species also remain unexplored. These bacteria are considered as 'brute force' pathogens that use multiple plant cell wall degrading enzymes, causing extensive tissue maceration in order to obtain nutrients from their host (Mäe *et al.* 2001; Perombelon 2002; Burr *et al.* 2006; Charkowski *et al.* 2012; Tarasova *et al.* 2013). From this point of view, it is difficult to contemplate that specific susceptible responses may be necessary for such a 'primitive' strategy of interaction. However, there are several prerequisites to consider the 'brute force' as not the only method of Pectobacterium interaction with the host. First, several genes that are typical of biotrophic pathogens (e.g. encoding type three secretion system proteins and phytotoxin coronatine biosynthetic enzymes) have been elucidated in the genomes of *Pectobacterium* species (Bell *et al.* 2004; Nikolaychik *et al.* 2014). Second, there are several observations that demonstrate the ability of plants and *Pectobacterium* to coexist for a long time without developing disease symptoms (Hayward 1974; Perombelon 2002; Czajkowski *et al.* 2011; Marquez-Villavicencio *et al.* 2011; Toth *et al.* 2011).

In our previous study, we also described the 'peculiar' behaviour of *P. atrosepticum* in tobacco plants that was not directly related to 'brute force' and occurred during the colonisation of xylem vessels (Gorshkov *et al.* 2014). We have shown that the extensive colonisation of the plant starts from the vessels, although intercellular spaces of the core parenchyma are considered to be the main niche for *Pectobacterium* within the host. In the vessels *P. atrosepticum* cells form specific multicellular structures, which we named 'bacterial emboli'. These structures totally occlude xylem vessels and provide the conditions for downward migration of the microorganisms. Bacterial emboli were also found in potato plants infected with *P. atrosepticum* (our unpublished data), and thus the formation of these structures likely represents a universal strategy of plant–*Pectobacterium* interactions.

The initial stages of bacterial emboli formation are not related to the attachment of microorganisms to the vessel wall, which is typical for bacterial biofilms described for phytopathogenic microorganisms (Purcell & Hopkins 1996; Koutsoudis *et al.* 2006; Danhorn & Fuqua 2007; Koczan *et al.* 2009; Baccari & Lindow 2011). The assemblage of bacterial emboli starts with the formation of a gel originating from substances accumulating on the inner surface of the vessel cell wall (Gorshkov *et al.* 2014). The formation of these substances, which are presumably released from plant cell wall (at least, as judged from electron microscopy), occurs prior to the intensive bacterial colonisation of the vessels, and thus cannot be attributed to the action of bacterial plant cell wall degrading enzymes.

The aim of the present study was to identify the components that comprise substances necessary for bacterial emboli formation and to trace the changes that occur in the xylem vessels of *P. atrosepticum*-infected plants during the colonisation of vessels by bacteria. Our working hypothesis was based on the possible penetration of the relatively high molecular weight products of degradation of plant cell wall polysaccharides into the lumen, where they provide xylem sap gelation necessary for the assembly of bacterial emboli; hence, the passage of the degradation products into the lumen is a result of a pathogen-induced response of the plant.

MATERIAL AND METHODS

Growth conditions for plants and bacteria and plant inoculation

Nicotiana tabacum cv. Havana plants were grown axenically in tubes in a growth chamber with a 16-h light/8-h dark cycle. Seeds were surface-sterilised using diluted bleach (0.8% active chlorine) and 1% sodium dodecyl sulphate for 30 min, washed seven times with sterile distilled water, then transferred to Murashige and Skoog medium (MS; Murashige & Skoog 1962) in Petri dishes. Ten-day-old seedlings were transferred to individual flasks containing MS.

A strain of *P. atrosepticum* SCRI1043 (formerly *Erwinia carotovora* subsp. *atroseptica* SCRI1043) was cultured in Luria–Bertani (LB) broth (Sambrook *et al.* 1989) on a rotary shaker (180 rpm) at 28 °C until the early stationary phase [2×10^9 colony-forming units ($CFU \cdot ml^{-1}$)]. Six to 7 weeks after planting, the stems of tobacco plantlets were inoculated with inoculum containing 2×10^7 $CFU \cdot ml^{-1}$. Sterile 10 mM $MgCl_2$ or bacterial suspension in 10 mM $MgCl_2$ containing 2×10^5 cells were placed as 10-μl drops on the surface of the plant stem without wounding the tissue. Samples of control and infected plants were taken for analysis with chromatography and microscopy 2 days after inoculation.

Preparation of buffer-extractable and ammonium oxalate-extractable cell wall fractions

The extraction of different fractions of polysaccharides was carried out from the stems of control or *P. atrosepticum*-infected plants or *P. atrosepticum* cells grown *in vitro*. A total of 1.2 g plant tissue or 1.2×10^{10} *P. atrosepticum* cells (the quantity that roughly exceeded five times the quantity of bacteria in 1.2 g infected tissue) were used as starting material. Samples were ground in liquid nitrogen in mortars. Five volumes of 50 mM Na/K-phosphate buffer (pH 7.0) were added to the obtained powders and the grinding continued until full thawing of the samples. The obtained homogenates were centrifuged for 10 min at 10,000 *g* and 4 °C. Then the supernatants containing buffer-extractable fractions were separated, incubated at 100 °C for 10 min and centrifuged for 10 min at 10,000 *g*, 4 °C. The buffer-extractable polysaccharides were precipitated from the supernatants with four volumes of 96% ethanol. Then the precipitates were harvested, washed three times with 80% ethanol and diluted in deionised water.

The pellets remaining after separation of the buffer-extractable fraction were resuspended in 80% ethanol, incubated at 100 °C for 10 min and harvested (10 min at 10,000 *g* and 4 °C). The pellets were washed with 80% ethanol, 50 mM Na/K-phosphate buffer and 100% acetone three times with each solution. For starch depletion, samples were treated twice with glucoamylase (Sigma, St. Louis, MO, USA) in phosphate buffer for 18–20 h each. Absence of starch in the samples was examined with KI-I_2 staining. After starch depletion, samples were washed with deionised water and acetone three times each and dried.

For extraction of ion-bound pectic compounds, the obtained cell wall pellets were suspended in 0.5% ammonium oxalate (pH 5.0) and incubated at 100 °C for 1 h. After centrifugation, the supernatants were collected and ammonium oxalate again added to the pellets followed by incubation at 100 °C for 1 h.

The supernatants obtained after both ammonium oxalate extractions were combined and polysaccharides precipitated by addition of four volumes 96% ethanol. The precipitates were then washed three times with 80% ethanol and dissolved in deionised water. The obtained buffer-extractable and ammonium oxalate-extractable fractions of cell walls were analysed using size-exclusion chromatography.

Size-exclusion chromatography

Size-exclusion chromatography of buffer-extractable and ammonium oxalate-extractable polysaccharides was carried out on a Sepharose CL-4B column (1.2 × 40 cm, Pharmacia, Uppsala, Sweden) using 0.01 M pyridine/acetic acid solution, pH 4.5, flow rate 0.25 ml·min^{-1}, fraction volume 1.0 ml. Pullulan samples of 1660, 380, 186, 100 and 48 kDa (Showa Denko, Tokyo, Japan) with low index of polydispersity (1.09–1.19) were used as standards for column calibration. Carbohydrate content in each fraction was measured using the phenol-sulphuric acid assay (Dubois *et al.* 1956).

Monosaccharide analysis

Polysaccharides of sub-fractions obtained after size-exclusion chromatography were hydrolysed with 2 M trifluoride acetic acid (TFA; Sigma) at 120 °C for 1 h and dried in a stream of air at 60 °C. Monosaccharide analysis was carried out with high performance anion-exchange chromatography (HPAEC) on a CarboPac PA-1 column (4 × 250 mm; Dionex, Sunnyvale, CA, USA), using pulse-amperometric detection (PAD; Dionex). Triple waveform B for the analysis of carbohydrates with ion chromatography using a gold working electrode was applied. Eluents: A – 0.015 M NaOH; B – 1 M NaOAc in 0.1 M NaOH. The column was equilibrated with eluent A – 100%. The sample was eluted with the following linear gradient: 0–20 min A – 100%; 20–21 min A – 90%, B – 10%; 21–31 min A – 70%, B – 30%; flow rate 1 ml·min^{-1} at 30 °C. Monosaccharide standards were treated with 2 M TFA at 120 °C 1 h before they were used for calibration.

The analysis of plant cell wall polysaccharides using size-exclusion chromatography and determination of monosaccharide content were performed in four independent biological replicates each. Within each sample, pieces of stems of ten to 12 plants were combined. The comparison was done using Wilcoxon signed rank test. A probability (P-value) of <0.05 was considered as statistically significant.

Immunocytochemistry assay

Sections of control and *P. atrosepticum*-infected tobacco stems (0.5–0.8-mm thick) were excised using a sterile razor blade 2 days after plant inoculation. The samples were fixed in a mixture of 2% paraformaldehyde and 0.5% glutaraldehyde prepared in 0.1 M phosphate buffer (pH 7.2) for 4 h at 4 °C. After washing, samples were post-fixed by incubation in 0.5% (w/v) osmium tetroxide diluted in 0.1 M phosphate buffer (pH 7.2) with sucrose (25 mg·ml^{-1}) at 4 °C for 1 h. Then samples were dehydrated in a graded aqueous ethanol series, transferred to 100% acetone and immersed in LR White resin (Medium Grade Acrylic Resin; Ted Pella, Redding, CA, USA; catalogue no. 18181) that contained acetone added in the proportions (v/v) 1:2, 1:1, 2:1, with each step involving a 12-h incubation. The samples were then embedded in LR White resin in Beem capsules and polymerised at 60 °C for 24 h.

Semi-thin sections (*ca.* 1-μm thick) were prepared using a glass knife on a LKB Ultracut III ultramicrotome, collected on silane-coated microscope slides and pre-incubated in Na-phosphate buffered saline (PBS), pH 7.4, containing 3% (w/v) bovine serum albumin (BSA) for 1 h to block non-specific labelling. The immunolabelling of pectic compounds was carried out using antibodies INRA-RU2 (Ralet *et al.* 2010), LM19 and LM20 (Verhertbruggen *et al.* 2009) specific to rhamnogalacturonan I, non-esterified and esterified homogalacturonan, respectively. The sections were incubated for 1 h with primary antibodies diluted (1:2 for INRA-RU2 and 1:10 for LM19 and LM20) in 0.1 M PBS containing 0.06% (w/v) BSA, washed three times with 0.1 M PBS and subsequently incubated for 1 h in the dark with goat anti-mouse antibody for INRA-RU2, goat anti-rat antibodies for LM19 and LM20, linked to fluorescein isothiocyanate (FITC; Sigma). The sections were then washed with Na-phosphate buffer and distilled water three times each and mounted in CFM-1 mountant solution (Electron Microscopic Sciences, Hatfield, PA, USA). All incubations were performed at room temperature. Primary antibodies were omitted in control experiments. Additionally, sections of bacterial cells grown *in vitro* were treated with the above used antibodies.

The sections were examined using a laser confocal fluorescence microscope (LSM 510 Meta; Carl Zeiss, Jena, Germany). Immunofluorescence was observed using excitation at 488 nm and emission at 503–550 nm. The transmitted light channel was used for detection of anatomical details.

Electron microscopy

Sections of plant stems (0.5–0.8-mm thick) were excised using a sterile razor blade on the second day after inoculation. The samples were fixed overnight in 2.5% glutaraldehyde prepared in 0.1 M phosphate buffer (pH 7.2) at 4 °C, washed three times with 0.1 M phosphate buffer containing sucrose (68 g·l^{-1}), and post-fixed by incubation in 1% (w/v) osmium tetroxide in the same buffer with sucrose (25 mg·ml^{-1}) at 4 °C for 4 h. The samples were dehydrated by passage through a graded ethanol series (30, 40, 50, 60, 70, 80, 90 and then 96% ethanol) before being transferred to 100% acetone and propylene oxide. Then the samples were immersed in Epon resin (Fluka, Buchs, Switzerland) that contained propylene oxide added in the proportions (v/v) 1:2, 1:1 and 2:1, with each step involving a 12-h incubation. The samples were then embedded in pure Epon resin.

Ultrathin sections (*ca.* 300 nm) were prepared using a glass knife on a LKB Ultracut III, mounted on copper grids and stained with 2% aqueous uranyl acetate (w/v) for 20 min and Reynolds' lead citrate (Reynolds 1963) for 7 min. The sections were examined using a transmission electron microscope (JEM-1200 EX; Jeol, Tokyo, Japan) operated at an accelerating voltage of 80 kV.

Analysis of reactive oxygen species (ROS)

To visualise ROS in the xylem vessels, sections of control and *P. atrosepticum*-infected plant stems (2 days after inoculation)

were incubated for 30 min in the presence of 10^{-5} M 2′,7′-dichlorofluorescin diacetate (DCF-DA; Sigma) prepared in 0.1 M phosphate buffer (pH 7.4). Then the sections were washed three times with the same buffer and observed under a laser confocal fluorescent microscope (LSM 510 Meta; Carl Zeiss) using an excitation wavelength of 488 nm and detection wavelengths between 503 and 550 nm.

All microscopy data comprise the reproducible results of two independent experiments, each with three biological replicates.

RESULTS

Analysis of degradation of plant cell wall polysaccharides during *P. atrosepticum*-induced infection

In order to characterise the changes in plant cell wall polysaccharides during *P. atrosepticum*-induced infection, size-exclusion chromatography of cell wall fractions was performed and elution profiles for control and infected plants compared. Emphasis was placed on the pectin-containing fractions: 50 mM phosphate buffer-extractable fraction that contained unbound or weakly bound cell wall polysaccharides and ammonium oxalate-extractable fraction that contained ion-bound pectins. Two main peaks represented the elution profile of the buffer-extractable fraction in *P. atrosepticum*-infected plants (Fig. 1a). The first peak contained polymers eluting in the region from 400 kDa to maximum in the 100 kDa region (according to column calibration with pullulans), and carbohydrates of < 50 kDa represented the second peak. The content of polymers in the buffer-extractable fraction of control plants was significantly lower and no pronounced peaks were observed on the elution profile of this fraction (Fig. 1a).

To verify that the increase in carbohydrate content in the buffer-extractable fraction of infected plants was due to the plant and not bacterial polysaccharides, a fraction prepared analogously was obtained from *P. atrosepticum* cells cultured *in vitro*. Although the quantity of bacteria used for extraction exceeded (roughly five-fold) the number of *P. atrosepticum* cells in infected plant samples prepared for the analysis, the content of carbohydrates in the buffer-extractable fraction of bacterial cells was almost six-fold less than that of infected plants (145 ± 24 and 836 ± 54 μg, respectively).

The elution profile of pectic polysaccharides from the ammonium oxalate-extractable fraction in control plants had a pronounced peak in a high molecular weight area (Fig. 1b); this peak was absent in the fraction obtained analogously from the infected plants. To check if the ion-bound pectins present

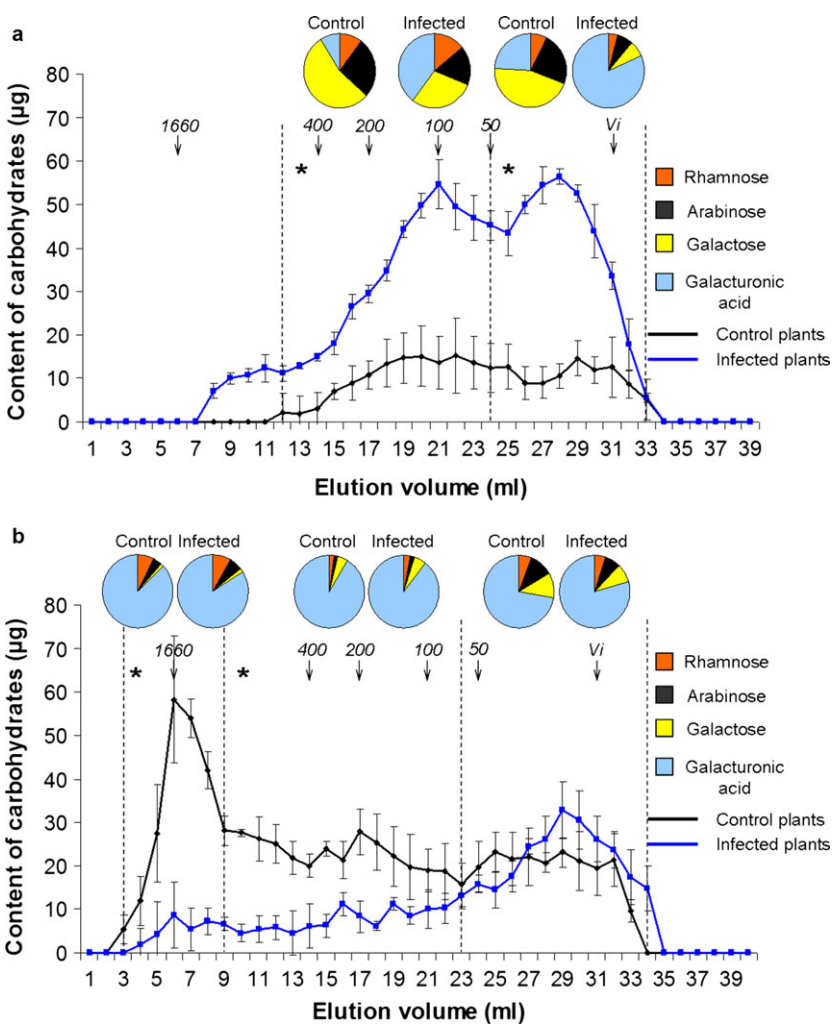

Fig. 1. Analysis of polysaccharides extracted with 50 mM phosphate buffer (a) or 0.5% ammonium oxalate (b) from the samples of stems of control (*black line*) or *P. atrosepticum*-infected (*blue line*) plants. Elution profiles (*lines*) were obtained using size-exclusion chromatography on a Sepharose CL-4B column; pullulans were used as molecular weight markers. Monosaccharide composition (*circle diagrams*) was analysed in different sub-fractions marked in the figure with vertical dotted lines. Samples of control and infected plants were equalised based on fresh weight. Values are means ± SD of four biological replicates. * – differences in carbohydrate content between sub-fractions of control and infected plants are significant ($P < 0.05$).

in the ammonium oxalate-extractable fraction of samples of control plants (Fig. 1b) gave rise to the polysaccharides that appeared in the buffer-extractable fraction of samples of infected plants (Fig. 1a), the analysis of monosaccharide composition was performed for polysaccharides of major sub-fractions of both fractions.

The bulk of the pectic compounds in the plant cell wall consists of homogalacturonan and rhamnogalacturonan I, which are usually linked together by covalent bonds (Fry 1998; Ridley *et al.* 2001). Homogalacturonan is a linear polymer built of galacturonic acid (GalA) residues. Rhamnogalacturonan I is a ramified polysaccharide, which contains GalA and rhamnose (Rha) in similar proportions in the backbone, and galactose (Gal) and/or arabinose (Ara) – in the side chains. Circle diagrams on top of elution profiles (Fig. 1a and b) and Table 1 present the composition of monosaccharides that are constituents of pectic compounds (GalA, Rha, Gal, Ara) in the sub-fractions (marked in Fig. 1a and b with vertical dotted lines) of buffer- and ammonium oxalate-extractable polysaccharide fractions obtained from control and infected plants. Pectins were the main polysaccharides of all analysed sub-fractions; the content of other minor monosaccharides detected (Glc, Xyl, GlcA) never exceeded 15%. The domination of blue sector (which marks GalA) in the circle diagram indicates that the sub-fraction is enriched in homogalacturonan, while the multicolour circles show the presence of significant amounts of neutral monosaccharides (Rha, Gal, Ara), and thus point to the enrichment of sub-fractions with rhamnogalacturonan I (Fig. 1a and b). The results of size-exclusion chromatography and analysis of monosaccharide composition show that in infected plants, a part of the ion-bound pectic compounds was transferred into the buffer-extractable fraction, indicating that they were released from plant cell wall. Hence, pectic compounds in the buffer-extractable fraction of infected plants were subdivided into two major sub-fractions that differed in monosaccharide composition (Fig. 1a). The polysaccharides of the relatively lower molecular weight sub-fraction consisted almost completely of GalA, while the sub-fraction eluting in the 100–400 kDa region was enriched in rhamnogalacturonan I (Fig. 1a). These fragments of pectic compounds are potentially able to form gels (Grant *et al.* 1973; Cardenas *et al.* 2008; Vithanage *et al.* 2010; Yapo & Gnakri 2015), and in the case of entering a xylem vessel, may provide the formation of a matrix for bacterial emboli.

Immunolocalisation of pectic polysaccharides in the xylem vessels during *P. atrosepticum*-induced infection

To verify whether the fragments of pectic compounds found in the buffer-extractable polysaccharide fraction of infected plants appeared inside the lumens of xylem vessels during *P. atrosepticum*-induced infection, an immunocytochemistry assay was performed using monoclonal antibodies INRA-RU2 specific to rhamnogalacturonan I (Ralet *et al.* 2010), LM19 and LM20 specific to non-esterified and esterified homogalacturonan, respectively (Verhertbruggen *et al.* 2009). On the cross-sections of control plants, INRA-RU2 (Fig. 2a), LM19 and LM20 (data not shown) antibodies tagged the intercellular spaces and middle lamella and no fluorescence was detected inside vessel lumens. The progression of *P. atrosepticum*-induced infection led to the appearance of substances in the lumens of primary vessels (Fig. 2b–h, indicated with *brown arrowheads*) that gave rise to the formation of a gel in which bacterial cells were trapped (Fig. 2i and j) resulting in the assembly of tight structures – bacterial emboli (Fig. 2k). These substances were not observed in the control plants. On the cross-sections of infected plants, LM19 and LM20 antibodies only labelled the middle lamella and intercellular spaces but not the substances released into the vessel lumen (Fig. 2b and c). In contrast, these substances were strongly tagged with INRA-RU2 antibodies (Fig. 2d, Fig. S1). The release of INRA-RU2-labelled substances became visible before bacterial cells were observed within the vessel lumen (Fig. 2d and f). As the bacteria appeared in the vessel (Fig. 2g) and the density of the *P. atrosepticum* population increased, the target substances became more and more loosened (Fig. 2h), forming a gel (Fig. 2i and j). At the stage of extensive vessel colonisation by bacteria, the degree of labelling of the vessel interior with INRA-RU2 decreased (Fig. 2d, marked with a *star*). This is likely related to dilution of rhamnogalacturonan I epitopes during the loosening of the

Table 1. Monosaccharide proportion (%) in different sub-fractions of buffer- and ammonium oxalate-extractable cell wall fractions of control and infected by *P. atrosepticum* tobacco plants.

fraction	sub-fraction [elution volume (ml)]	sample	Rha (%)	Ara (%)	Gal (%)	GalA (%)
buffer-extractable	12–23	control	10.3 ± 1.4^{a}	26.4 ± 1.3^{a}	$54.4 \pm 2.2^{a,b}$	$8.9 \pm 1.9^{a,b}$
		infected	$14.2 \pm 1.1^{a,b}$	$16.8 \pm 2.9^{a,b}$	$29.3 \pm 0.9^{a,b}$	$39.7 \pm 1.7^{a,b}$
	24–33	control	7.5 ± 4.1	23.4 ± 4.1^{a}	$45.1 \pm 3.6^{a,b}$	$24.0 \pm 2.9^{a,b}$
		infected	4.3 ± 0.2^{b}	$7.1 \pm 0.6^{a,b}$	$6.9 \pm 0.5^{a,b}$	$81.7 \pm 1.2^{a,b}$
oxalate-extractable	3–9	control	7.4 ± 1.0	4.3 ± 1.8	1.2 ± 0.5	87.1 ± 3.2
		infected	8.4 ± 1.2	6.1 ± 1.8	1.6 ± 0.5	83.9 ± 2.4
	10–22	control	2.2 ± 0.8	1.6 ± 1.2	4.8 ± 0.5	91.4 ± 2.2
		infected	3.0 ± 0.4	2.0 ± 0.5	5.5 ± 1.7	89.5 ± 2.5
	23–34	control	5.8 ± 1.7	11.0 ± 3.5	10.9 ± 0.9^{a}	72.3 ± 5.2
		infected	5.1 ± 2.3	7.2 ± 1.1	8.2 ± 1.7^{a}	79.5 ± 1.9

Values are means ± SD of four biological replicates.

[a]Differences between samples of control and infected plants are significant.

[b]Differences between sub-fractions of buffer-extractable polysaccharides eluting in 12–23 ml and 24–33 ml are significant. Significance was analysed using Wilcoxon signed rank test ($P < 0.05$).

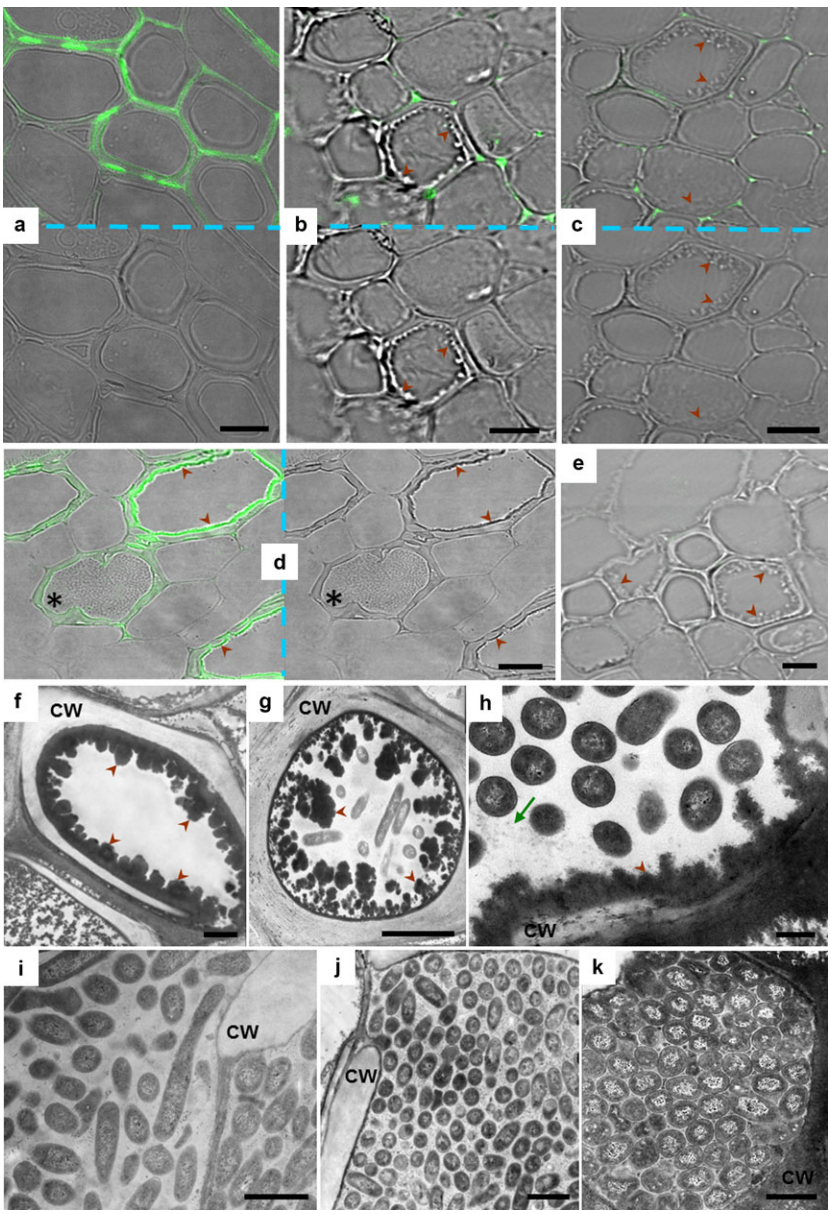

Fig. 2. Sections of control (a) or infected with *P. atrosepticum* (b–k) tobacco plants: indirect immunofluorescence detection of rhamnogalacturonan I and homogalacturonan epitopes (a–e) or transmission electron microscopy (f–k). a – sections of control plants treated with INRA-RU2. b, c, d – sections of infected plants treated with LM19, LM20 and INRA-RU2, respectively. Sections a–d are in both bright and green/bright fields. e – section of infected plants treated with secondary, but not primary, antibody (given only in green/bright field). Monoclonal antibodies INRA-RU2, LM19 and LM20 are specific to rhamnogalacturonan I, non-esterified and esterified homogalacturonan, respectively. f – release of the substance from the plant cell wall (note that no bacteria are present in vessel). g, h – gradual loosening of the substance released from the plant cell wall as the bacteria appear in the vessel and their population density increases. i, j – formation of a gel that consolidates the bacterial cells. k – total occlusion of the vessel by bacterial emboli. *Star* on section d marks lumen extensively colonised with *P. atrosepticum* not tagged with INRA-RU2 in contrast to non- or weakly colonised neighbouring vessels. Scale bars are 10 μm in a–e and g, 2 μm in f and j, 0.5 μm in h, 1 μm in i and k. CW – plant cell wall. *Brown arrowheads* mark substances released from cell walls of primary xylem vessels; *green arrow* shows loosening of the substance.

target substances and formation of the gel and/or gradual destruction of this polysaccharide by enzymes produced from the increasing number of bacterial cells. No fluorescence was observed when the cross-sections were incubated with secondary but without primary antibodies (Fig. 2e). Bacterial cells grown *in vitro* were not tagged with the used antibodies (data not shown). Thus, our results demonstrate that colonisation of the primary xylem vessels and formation of bacterial emboli were preceded by the release of rhamnogalacturonan I from the plants cell walls into the lumen of the vessels.

Analysis of ROS in the xylem vessels of *P. atrosepticum*-infected plants

Since no bacteria were observed in the lumen of the primary xylem vessels when rhamnogalacturonan I started to be released from the plant cell walls into the lumen, this process is suggested to be a result of vessel wall modification in the framework of the pathogen-induced response of the plant. The change in the plant cell wall, coupled with the decay of matrix polysaccharides is caused by ROS. ROS were demonstrated to lead to non-enzymatic fragmentation of pectins and cross-linking glycans (Fry *et al.* 2001; Schopfer 2001; Müller *et al.* 2009). Therefore, we examined whether colonisation of the xylem vessels by *P. atrosepticum* was coupled with an increase in ROS. To compare levels of ROS in the vessels of control and *P. atrosepticum*-infected plants a fluorescent dye, DCF-DA, was used.

In control plants, only weak fluorescence was detected in the cell walls of secondary xylem vessels and no fluorescence was visible in the primary xylem (Fig. 3a). In contrast, primary vessels of infected plants were highly stained (Fig. 3b, Fig. S2). The intensity of fluorescence of the secondary xylem vessels in infected plants was comparable to that of control plants (Fig. 3a and b). Walls of primary vessels in infected plants displayed strong fluorescence prior to their intensive colonisation

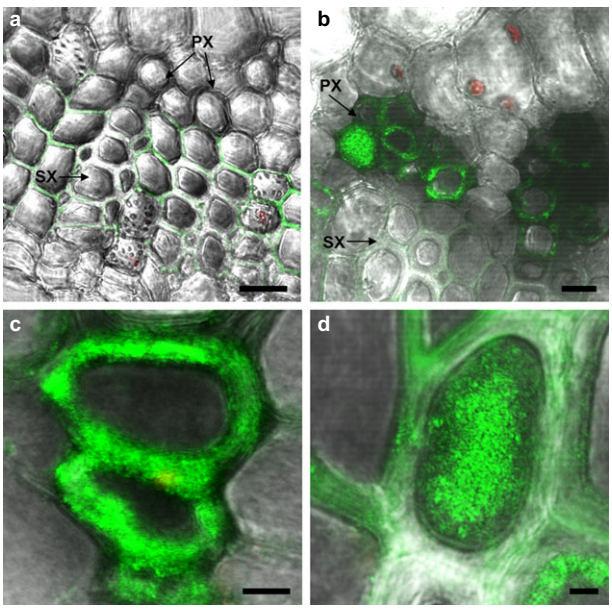

Fig. 3. Fluorescence microscopy imaging of ROS in tobacco plants using DCF-DA. The pictures show DCF-DA-stained sections of non-infected (a) or *P. atrosepticum*-infected (b–d) plants. Non-colonised and colonised vessels are shown in c and d, respectively. Scale bars correspond to 20, 20, 2, 5 μm for a–d, respectively. PX – primary xylem vessels. SX – secondary xylem vessels.

by bacteria (Fig. 3b and c). As the density of bacterial cells within the vessel increased, the intensity of fluorescence of the cell wall decreased and the lumen of the vessels became stained (Fig. 3b and d). Thus, the assembly of bacterial emboli that are formed only in primary, but not the secondary, xylem vessels follows an increase in ROS levels in the primary vessels.

DISCUSSION

In the present study, we have shown that the formation of bacterial emboli in *P. atrosepticum*-infected tobacco plants is preceded by significant changes in the primary xylem vessels. The colonisation of the primary vessels by bacteria follows the appearance of pectic fragments (rhamnogalacturonan I) in the lumen. These fragments originate from the high molecular weight pectic compounds of the ammonium oxalate-extractable fraction of the plant cell wall and give rise to a gel that is involved in bacterial emboli assembly.

The formation of gels in the vessels of plants infected by various pathogens has previously been shown and was attributed to either action of the pathogen's plant cell wall degrading enzymes or the host's defence response that hampered systemic spread of the parasite (Hilaire *et al.* 2001; Yadeta & Thomma 2013). In our study, the penetration of pectic polymers into the lumen started before extensive colonisation by the pathogen and thus could not be explained as the activity of *Pectobacterium* enzymes. As neither the bacterial damage nor the localisation of the infection site were caused by the substances released from the plant cell wall (Gorshkov *et al.* 2014), this refutes their defensive role against *P. atrosepticum* infection. It is possible that gelation of the xylem sap is a defence response that may be effective against specific pathogens but is not effective against others, including *P. atrosepticum*.

To interact with the plant, microbial cells must coordinate, communicating with each other through mediators or cell contacts (Danhorn & Fuqua 2007; Liu *et al.* 2008; Newman *et al.* 2008). Xylem sap flow may negatively effect microbial communication, creating 'chaos' within the vessel-colonising (sub) population. Many plant pathogens can withstand this inconvenience by forming ordered structures – biofilms – inside the xylem vessels that enable the bacteria to anchor in a particular place and communicate with each other. Biofilm formation converts individual autonomous bacterial cells into a 'multicellular' structure that is known to be necessary for realisation of specific physiological programmes, including those that determine the ability to interact with the host plant (Sutherland 2001; Danhorn & Fuqua 2007; Stoodley & Stoodley 2009). The bacterial attachment is a known initial and crucial stage in biofilm formation during the colonisation of xylem vessels by various plant pathogenic bacteria (Bogs *et al.* 1998; Newman *et al.* 2004; Koutsoudis *et al.* 2006; Koczan *et al.* 2009). However, we did not observe *P. atrosepticum* attachment to the walls of xylem vessels prior to the formation of bacterial emboli (Gorshkov *et al.* 2014; this study). This is consistent with the poor attachment and biofilm-forming capacities of *P. atrosepticum* that have previously been observed (Perez-Mendoza *et al.* 2011). Nevertheless, this bacterium is able to form highly ordered biofilm-like structures in the vessels – bacterial emboli. In contrast to biofilms, formation of bacterial emboli does not require cell attachment. As an alternative, *P. atrosepticum* cells gain a foothold in a particular area of the xylem vessel through gelation of xylem sap from plant-derived polysaccharides. Thus, our results demonstrate that *P. atrosepticum* uses metabolites of the plant not only as a nutrient source but also as building material in order to form a structured community within the xylem vessels.

Detection of pectic compounds within the xylem vessels in infected plants raises a question about the way these polysaccharides enter the vessel lumen from the plant cell wall. We suggest that the appearance of pectic compounds in xylem vessels during infection is a result of their excision from plant cell walls due to the pathogen-induced increase in ROS. ROS are known to cause non-enzymatic fragmentation of various polysaccharides, including those of the plant cell wall, both *in vitro* and *in planta*, resulting in modification of properties of the plant cell wall (Fry *et al.* 2001; Schopfer 2001; Müller *et al.* 2009). In our experiments, we found that *P. atrosepticum*-induced infection led to generation of ROS in the cell walls of primary xylem vessels. This increase in ROS became evident at the time of penetration of pectic polymers into the lumen prior to the extensive colonisation by the bacteria.

The generation of ROS is generally accepted as a pathogen-induced defence response that restricts or eliminates the parasite within host tissues. However, we did not find any evidence that an increase in ROS hampered the propagation of *P. atrosepticum* in the xylem vessels. These results are in accordance with previously published data for bacteria closely related to *P. atrosepticum*, i.e. the phytopathogenic bacterium *Erwinia chrisanthemi* (*Dickeya dadantii*). This bacterium was proved to be resistant to host-derived ROS (Miguel *et al.* 2000; Reverchon *et al.* 2002; Asselbergh *et al.* 2008).

The formation of bacterial emboli such as the reactions described in the present study (penetration of rhamnogalacturonan I into the lumen and generation of ROS) occurred site-specifically – in the primary xylem vessels; these processes were not observed in secondary xylem or other plant tissues. This indicates that the formation of bacterial emboli requires specific host reactions that proceed only in the primary xylem vessels. These reactions may be regarded as a part of the host's susceptible response, since they did not restrict the infection but contrarily contributed to colonisation of the plant. Both pathogen-associated molecular pattern and *Pectobacterium*-derived specific signalling molecules, which serve as manipulators of host behaviour, might induce the increase in ROS and accumulation of rhamnogalacturonan I in the lumen of primary xylem vessels during the *Pectobacterium*–tobacco interaction. However, the inducers of this kind of susceptible response remain to be revealed.

Taken together our results demonstrate that colonisation of the plant by *P. atrosepticum* is coupled with the host's susceptible response that occurs in primary xylem vessels and includes generation of ROS and penetration of rhamnogalacturonan I fragments into the lumen. These reactions precede colonisation of the vessels by bacteria and serve as the basis for the assembly of bacterial emboli. Bacterial emboli thus represent the products of the host–pathogen integration, since the formation of these structures requires the action of both partners.

ACKNOWLEDGEMENTS

We would like to express our gratitude to Professor Paul Knox (University of Leeds, UK) for LM19 and LM20 antibodies and Dr Fabienne Guillon (INRA, France) for the INRA-RU2 antibody. This study was supported in part by the Russian Foundation for Basic Research, (project Nos. 14-04-01750-a, 14-04-01828-a), and a grant (MK-7359.2015.4) from the President of the Russian Federation for Young Scientists. Analysis of ROS was supported through the Russian Science Foundation (project No. 15-14-10022).

SUPPORTING INFORMATION

Additional Supporting Information may be found online in the supporting information tab for this article:

Figure S1. Immunofluorescence detection of rhamnogalacturonan I in *P. atrosepticum*-infected tobacco plants using INRA-RU2 antibodies (replicates similar to Fig. 2d of main text). Sections are given in both bright and green/bright fields. Scale bars: 20 μm in a, 10 μm in b–d, 5 μm in e.

Figure S2. Fluorescence microscopy imaging of ROS in *P. atrosepticum*-infected tobacco plants using DCF-DA (replicates similar to Fig. 3b–d of main text). Scale bars correspond to 20 (a, b), 10 (c, e), 5 (d, f) μm.

REFERENCES

Able A.J. (2003) Role of reactive oxygen species in the response of barley to necrotrophic pathogens. *Protoplasma*, **221**, 137–143.

Agrios G.N. (2005) *Plant pathology*, 5th edition. Elsevier, London, UK pp 922.

Asselbergh B., Achuo A.E., Höfte M., Gijsegem F.V. (2008) Abscisic acid deficiency leads to rapid activation of tomato defence responses upon infection with *Erwinia chrysanthemi*. *Molecular Plant Pathology*, **9**, 11–24.

Baccari C., Lindow S.E. (2011) Assessment of the process of movement of *Xylella fastidiosa* within susceptible and resistant grape cultivars. *Phytopathology*, **101**, 77–84.

Bain R.A., Perombelon M.C.M., Tsror L., Nachmias A. (1990) Blackleg development and tuber yield in relation to numbers of *Erwinia carotovora* subsp. *atroseptica* on seed tubers. *Plant Pathology*, **39**, 125–133.

Bell K.S., Sebaihia M., Pritchard L., Holden M.T.G., Hyman L.J., Holeva M.C., Thomson N.R., Bentley S.D., Churcher L.J.C., Mungall K., Atkin R., Bason N., Brooks K., Chillingworth T., Clark K., Doggett J., Fraser A., Hance Z., Hauser H., Jagels K., Moule S., Norbertczak H., Ormond D., Price C., Quail M.A., Sanders M., Walker D., Whitehead S., Salmond G.P.C., Birch P.R.J., Parkhill J., Toth I.K. (2004) Genome sequence of the enterobacterial phytopathogen *Erwinia carotovora* subsp. *atroseptica* and characterization of virulence factors. *Microbiology*, **101**, 11105–11110.

Bogs J., Bruchmüller I., Erbar C., Geider K. (1998) Colonization of host plants by the fire blight pathogen *Erwinia amylovora* marked with genes for bioluminescence and fluorescence. *Phytopathology*, **88**, 416–421.

Burr T., Barnard A.M.L., Corbett M.J., Pemberton C.L., Simpson N.J.L., Salmond G.P.C. (2006) Identification of the central quorum sensing regulator of virulence in the enteric phytopathogen, *Erwinia carotovora*: the VirR repressor. *Molecular Microbiology*, **59**, 113–125.

Cardenas A., Goycoolea F.M., Rinaudo M. (2008) On the gelling behaviour of 'nopal' (*Opuntia ficus indica*) low methoxyl pectin. *Carbohydrate Polymers*, **73**, 212–222.

Charkowski A., Blanco C., Condemine G., Expert D., Franza T., Hayes C., Hugouvieux-Cotte-Pattat N., Solanilla E.L., Low D., Moleleki L., Pirhonen M., Pitman A., Perna N., Reverchon S., Rodr′ıguez Palenzuela P., Francisco M.S., Toth I., Tsuyumu S., van der Waals J., van der Wolf J., Gijsegem F.V., Yang C.-H., Yedidia I. (2012) The role of secretion systems and small molecules in soft-rot *Enterobacteriaceae* pathogenicity. *Annual Review of Phytopathology*, **50**, 21.1–25.25.

Cui J., Bahrami A.K., Pringle E.G., Hernandez-Guzman G., Bender C.L., Pierce N.E., Ausubel F.M. (2005) *Pseudomonas syringae* manipulates systemic plant defenses against pathogens and herbivores. *Proceedings of the National Academy of Sciences of the United States of America*, **102**, 1791–1796.

Czajkowski R., Perombelon M.C.M., van Veen J.A., van der Wolf J.M. (2011) Control of blackleg and tuber soft rot of potato caused by *Pectobacterium* and *Dickeya* species: a review. *Plant Pathology*, **60**, 999–1013.

Danhorn T., Fuqua C. (2007) Biofilm formation by plant-associated bacteria. *Annual Review of Microbiology*, **61**, 401–422.

Ding X., Cao Y., Huang L., Zhao J., Xu C., Li X., Wang S. (2008) Activation of the indole-3-acetic acid–amido synthetase GH3-8 suppresses expansin expression and promotes salicylate- and jasmonate-independent basal immunity in rice. *The Plant Cell*, **20**, 228–240.

Dodds P.N., Rathjen J.P. (2010) Plant immunity: towards an integrated view of plant–pathogen interactions. *Nature Reviews Genetics*, **11**, 539–548.

Dubois M., Gilles K.A., Hamilton J.K., Rebers P.A., Smith F. (1956) Colorimetric method for determination of sugars and related substances. *Analytical Chemistry*, **28**, 350–356.

Efetova M., Zeier J., Riederer M., Lee C.-W., Stingl N., Mueller M., Hartung W., Hedrich R., Deeken R. (2007) A central role of abscisic acid in drought stress protection of *Agrobacterium*-induced tumors on Arabidopsis. *Plant Physiology*, **145**, 853–862.

Fry S.C. (1998) Oxidative scission of plant cell wall polysaccharides by ascorbate-induced hydroxyl radicals. *The Biochemical Journal*, **332**, 507–515.

Fry S.C., Dumville J.C., Miller J.G. (2001) Fingerprinting of polysaccharides attacked by hydroxyl radicals *in vitro* and in the cell walls of ripening pear fruit. *The Biochemical Journal*, **357**, 729–737.

Gorshkov V., Daminova A., Ageeva M., Petrova O., Gogoleva N., Tarasova N., Gogolev Y. (2014) Dissociation of a population of *Pectobacterium atrosepticum* SCRI1043 in tobacco plants: formation of bacterial emboli and dormant cells. *Protoplasma*, **251**, 499–510.

Govrin E.M., Levine A. (2000) The hypersensitive response facilitates plant infection by the necrotrophic pathogen *Botrytis cinerea*. *Current Biology*, **10**, 751–757.

Grant G.T., Morris E.R., Rees D.A., Smith P.J., Thom D. (1973) Biological interactions between polysaccharides and divalent cations: the egg-box model. *FEBS Letters*, **32**, 195–198.

Greenberg J.T., Silverman F.P., Liang H. (2000) Uncoupling salicylic acid-dependent cell death and defense-related responses from disease resistance in

the Arabidopsis mutant acd5. *Genetics*, **156**, 341–350.

Hayward C. (1974) Latent infections by bacteria. *Annual Review of Phytopathology*, **12**, 87–97.

Hilaire E., Young S.A., Willard L.H., McGee J.D., Sweat T., Chittoor J.M., Guikema J.A., Leach J.E. (2001) Vascular defense responses in rice: peroxidase accumulation in xylem parenchyma cells and xylem wall thickening. *Molecular Plant-Microbe Interactions*, **14**, 1411–1419.

Hirsch J., Deslandes L., Feng D.X., Balagué C., Marco Y. (2002) Delayed symptom development in *ein2-1*, an *Arabidopsis* ethylene-insensitive mutant, in response to bacterial wilt caused by *Ralstonia solanacearum*. *Phytopathology*, **92**, 1142–1148.

Koczan J.M., McGrath M.J., Zhao Y., Sundin G.W. (2009) Contribution of *Erwinia amylovora* exopolysaccharides amylovoran and levan to biofilm formation: implications in pathogenicity. *Phytopathology*, **99**, 1237–1244.

Koutsoudis M.D., Tsaltas D., Minogue T.D., von Bodman S.B. (2006) Quorum-sensing regulation governs bacterial adhesion, biofilm development, and host colonization in *Pantoea stewartii* subspecies *stewartii*. *Proceedings of the National Academy of Sciences of the United States of America*, **103**, 5983–5988.

Laurie-Berry N., Joardar V., Street I.H., Kunkel B.N. (2006) The *Arabidopsis thaliana Jasmonate insensitive 1* gene is required for suppression of salicylic acid-dependent defenses during infection by *Pseudomonas syringae*. *Molecular Plant-Microbe Interactions*, **19**, 789–800.

Liu H., Coulthurst S.J., Pritchard L., Hedley P.E., Ravensdale M., Humphris S., Burr T., Takle G., May-Bente B., Birch P.R.J., Salmond G.P.C., Toth I.K. (2008) Quorum sensing coordinates brute force and stealth modes of infection in the plant pathogen *Pectobacterium atrosepticum*. *PLoS Pathogens*, **4**, 1–11.

Lorang J.M., Sweat T.A., Wolpert T.J. (2007) Plant disease susceptibility conferred by a 'resistance' gene. *Proceedings of the National Academy of Sciences of the United States of America*, **104**, 14861–14866.

Lund S.T., Stall R.E., Klee H.J. (1998) Ethylene regulates the susceptible response to pathogen infection in tomato. *The Plant Cell*, **10**, 371–382.

Mäe A., Montesano M., Koiv V., Palva E.T. (2001) Transgenic plants producing the bacterial pheromone *N*-acyl-homoserine lactone exhibit enhanced resistance to the bacterial phytopathogen *Erwinia carotovora*. *Molecular Plant-Microbe Interactions*, **14**, 1035–1042.

Marquez-Villavicencio M.D.P., Groves R.L., Charkowski A.O. (2011) Soft rot disease severity is affected by potato physiology and *Pectobacterium* taxa. *Plant Disease*, **95**, 232–241.

Mauch-Mani B., Mauch F. (2005) The role of abscisic acid in plant–pathogen interactions. *Current Opinion in Plant Biology*, **8**, 409–414.

Miguel E., Poza-Carrión C., López-Solanilla E., Aguilar I., Llama-Palacios A., García-Olmedo F., Rodríguez-Palenzuela P. (2000) Evidence against a direct antimicrobial role of H_2O_2 in the infection of plants by *Erwinia chrysanthemi*. *Molecular Plant-Microbe Interactions*, **13**, 421–429.

Müller K., Linkies A., Vreeburg R.A., Fry S.C., Krieger-Liszkay A., Leubner-Metzger G. (2009) *In vivo* cell wall loosening by hydroxyl radicals during cress seed germination and elongation growth. *Plant Physiology*, **150**, 1855–1865.

Murashige T., Skoog F. (1962) A revised medium for rapid growth and bio assays with tobacco tissue cultures. *Physiologia Plantarum*, **15**, 473–497.

Navarro L.A., Dunoyer P., Jay F., Arnold B., Dharmasiri N., Estelle M., Voinnet O., Jones J.D.G. (2006) Plant miRNA contributes to antibacterial resistance by repressing auxin. *Science*, **312**, 436–439.

Newman K.L., Almeida R.P.P., Purcell A.H., Lindow S.E. (2004) Cell–cell signaling controls *Xylella fastidiosa* interactions with both insects and plants. *Proceedings of the National Academy of Sciences of the United States of America*, **101**, 1737–1742.

Newman K.L., Chatterjee S., Ho K.A., Lindow S.E. (2008) Virulence of plant pathogenic bacteria attenuated by degradation of fatty acid cell-to-cell signaling factors. *Molecular Plant-Microbe Interactions*, **21**, 326–334.

Nickstadt A., Thomma B.P.H.J., Feussner I.V., Kangasjarvi J., Zeier J., Loeffler C., Scheel D., Berger S. (2004) The jasmonate-insensitive mutant *jin1* shows increased resistance to biotrophic as well as necrotrophic pathogens. *Molecular Plant Pathology*, **5**, 425–434.

Nikolaychik Y., Gorshkov V., Gogolev Y., Valentovich L., Evtushenkov A. (2014) Genome sequence of *Pectobacterium atrosepticum* strain 21A. *Genome Announcements*, **2**, e00935-14.

O'Donnell P.J., Jones J.B., Antoine F.R., Ciardi J., Klee H.J. (2001) Ethylene-dependent salicylic acid regulates an expanded cell death response to a plant pathogen. *The Plant Journal*, **25**, 315–323.

O'Donnell P.J., Schmelz E.A., Moussatche P., Lund S.T., Jones J.B., Klee H.J. (2003a) Susceptible to intolerance – a range of hormonal actions in a susceptible *Arabidopsis* pathogen response. *The Plant Journal*, **33**, 245–257.

O'Donnell P.J., Schmelz E., Block A., Miersch O., Wasternack C., Jones J.B., Klee H.J. (2003b) Multiple hormones act sequentially to mediate a susceptible tomato pathogen defense response. *Plant Physiology*, **133**, 1181–1189.

Perez-Mendoza D., Coulthurst S.J., Sanjua′n J., Salmond G.P.C. (2011) N-Acetylglucosamine-dependent biofilm formation in *Pectobacterium atrosepticum* is cryptic and activated by elevated c-di-GMP levels. *Microbiology*, **157**, 3340–3348.

Perombelon M.C.M. (2002) Potato diseases caused by soft rot erwinias: an overview of pathogenesis. *Plant Pathology*, **51**, 1–12.

Purcell A.H., Hopkins D.L. (1996) Fastidious xylem-limited bacterial plant pathogens. *Annual Review of Phytopathology*, **34**, 131–151.

Ralet M.C., Tranquet O., Poulain D., Moïse A., Guillon F. (2010) Monoclonal antibodies to rhamnogalacturonan I backbone. *Planta*, **231**, 1373–1383.

Reverchon S., Rouanet C., Expert D., Nasser W. (2002) Characterization of indigoidine biosynthetic genes in *Erwinia chrysanthemi* and role of this blue pigment in pathogenicity. *Journal of Bacteriology*, **184**, 654–665.

Reynolds E.S. (1963) The use of lead citrate at high pH as an electron opaque stain in electron microscopy. *Journal of Cell Biology*, **17**, 208–212.

Ridley B.L., O'Neill M.A., Mohnen D. (2001) Pectins: structure, biosynthesis, and oligogalacturonide-related signaling. *Phytochemistry*, **57**, 929–967.

Robert-Seilaniantz A., Navarro L., Bari R., Jones J.D.G. (2007) Pathological hormone imbalances. *Current Opinion in Plant Biology*, **10**, 372–379.

Sambrook J., Fritsch E.F., Maniatis T. (1989) *Molecular cloning: a laboratory manual*, 2nd edition. Cold Spring Harbor Press, Cold Spring Harbor, New York, USA pp 1626

Schopfer P. (2001) Hydroxyl radical-induced cell-wall loosening *in vitro* and *in vivo*: implications for the control of elongation growth. *The Plant Journal*, **28**, 679–688.

Shan X.C., Goodwin P.H. (2006) Silencing an ACC oxidase gene affects the susceptible host response of *Nicotiana benthamiana* to infection by *Colletotrichum orbiculare*. *Plant Cell Reports*, **25**, 241–247.

Spoel S.H., Dong X. (2012) How do plants achieve immunity? Defence without specialized immune cells. *Nature Reviews Immunology*, **12**, 89–100.

Stoodley L.H., Stoodley P. (2009) Evolving concepts in biofilm infections. *Cellular Microbiology*, **11**, 1034–1043.

Sutherland I.W. (2001) The biofilm matrix – an immobilized but dynamic microbial environment. *Trends in Microbiology*, **9**, 222–227.

Tarasova N., Gorshkov V., Petrova O., Gogolev Y. (2013) Potato signal molecules that activate pectate lyase synthesis in *Pectobacterium atrosepticum* SCRI1043. *World Journal of Microbiology & Biotechnology*, **29**, 1189–1196.

Thatcher L.F., Manners J.M., Kazan K. (2009) *Fusarium oxysporum* hijacks COI1-mediated jasmonate signaling to promote disease development in Arabidopsis. *The Plant Journal*, **58**, 927–939.

Toth I.K., Bell K.S., Holeva M.C., Birch P.R.J. (2003) Soft rot erwiniae: from genes to genomes. *Molecular Plant Pathology*, **4**, 17–30.

Toth I.K., van der Wolf J.M., Saddler G., Lojkowska E., Helias V., Pirhonen M., Tsror L. (Lahkim), Elphinston J.G. (2011) *Dickeya* species: an emerging problem for potato production in Europe. *Plant Pathology*, **60**, 385–399.

Uehara T., Sugiyama S., Matsuura H., Arie T., Masuta C. (2010) Resistant and susceptible responses in tomato to cyst nematode are differentially regulated by salicylic acid. *Plant and Cell Physiology*, **51**, 1524–1536.

Verhertbruggen Y., Marcus S.E., Haeger A., Ordaz-Ortiz J.J., Knox J.P. (2009) An extended set of monoclonal antibodies to pectic homogalacturonan. *Carbohydrate Research*, **344**, 1858–1862.

Vithanage C.R., Grimson M.J., Wills P.R., Harrison P., Smith B.G. (2010) Rheological and structural properties of high methoxyl esterified, low methoxyl esterified and low methoxylamidated pectin gels. *Journal of Texture Studies*, **41**, 899–927.

Vogel J., Raab T.K., Schiff C., Somerville S.C. (2002) *PMR6*, a pectate lyase-like gene required for powdery mildew susceptibility in Arabidopsis. *The Plant Cell*, **14**, 2095–2106.

Yadeta K.A., Thomma B.P.H.J. (2013) The xylem as battleground for plant hosts and vascular wilt pathogens. *Frontiers in Plant Science*, **4**, 1–12.

Yapo B.M., Gnakri D. (2015) Pectic polysaccharides and their functional properties. In: Ramawat K.G., Merillon J.-M. (Eds) *Polysaccharides*. Springer International Publishing, Switzerland, pp 1729–1749.

Zheng X.-Y., Spivey N.W., Zeng W., Liu P.-P., Fu Z.Q., Klessig D.F., He S.Y., Dong X. (2012) Coronatine promotes *Pseudomonas syringae* virulence in plants by activating a signaling cascade that inhibits salicylic acid accumulation. *Cell Host & Microbe*, **11**, 587–596.